Internal Structural Imaging of Cultural Wooden Relics Based on Three-Dimensional Computed Tomography

Guiling Zhao,[a,b] Zhaowen Qiu, [a,]* Jun Shen,[a,]* Zhongji Deng,[a] Jinghua Gong,[c] and Dan Liu [b]

An efficient method for the internal structural imaging of cultural wooden relics was explored through experimental techniques of three-dimensional (3-D) tomography and reconstruction. The techniques of filtering and segmentation were applied to the 3-D scanned data of wooden cultural relics.To obtain high resolution 3D data model, it was necessary to preprocess the raw data after CT scanning. Preprocessing included denoising, filtering, and segmentation. After completing these three steps, three-dimensional reconstruction experiments were carried out (including surface rendering and volume rendering). After the 3-D reconstruction, the wood internal properties were visually analyzed and used to create internal structural imaging of wooden artifacts. On the basis of volume rendering, wooden artifacts could be graphically divided at any angle and any position. The textures of local wooden relics were clearly revealed in the segmentation of the reconstruction pictures, and these were compared with the presented internal structural image testing of the wooden artifacts. This study showed that the proposed technology can successfully create internal structural images of wooden artifacts, as well as provide important data and models to support the renovation and recovery of the cultural wooden relics.

Keywords: Three-dimensional cultural wooden relics segmentation; Computed tomography; Total variation; Three-dimensional reconstruction

*Contact information: a. Key Laboratory of Bio-based Materials Science and Technology of Ministry of Education, information and the College of Computer Engineering, Northeast Forestry University, Harbin, P.R. China, 150040; b: Art Academy, Northeast Agricultural University Harbin, China, 150040; c: Department of Science and Environmental Studies, Faculty of Liberal Arts and Social Sciences, Education University of Hong Kong; *Corresponding authors: 3256073977@qq.com;28329061@qq.com*

INTRODUCTION

Currently, three-dimensional (3-D) tomography technology is mainly used in the medical field but not in the protection and identification of wooden artifacts. However, there are some studies utilizing structural imaging technology in wood. Kak and Slaney (1988) used computed temography (CT) to analyze and graph X-ray detection results. Schmoldt *et al.* (1999) visualized the internal structure of wood with X-rays; the initial approach only contained one signal detector, and the wood had to be constantly moved. Ekevad (2004) described a CT-directional method where the fiber directions of wood in 3-D space were calculated from the pixel information on a series of two-dimensional (2-D) computed tomography images. This CT-directional method is a nondestructive way to measure fiber directions locally and in the interior of a piece of wood. Sarigul *et al*. (2005) developed the IntelliPost model system to improve the CT detection ability of wood defects. This system contained a learning model and an operation model. The learning model included wood defects identified by the operating equipment and established a system imaging rules for defects. The operational model discriminated the defects automatically based on the learning model. This system can be applied to inspect wood from different trees.

CT coupled with artificial neural network technology has allowed nondestructive tests on wood through structural imaging technology. The feed-forward back-propagation artificial neural network is the most efficient CT image processing method (Wei *et al*. 2011). Other studies have attemped to reconstruct 3-D logs or board images from two-dimensional (2-D) CT images, but there have been no studies of 3-D reconstruction. Mikolajska *et al*. (2012) described the difference between neutron and X-ray photon-based radiographic technologies. Brodersen (2013) discussed the origins of xylem reconstructions using traditional methods, current applications of mu CT in plant biology, and pertinent technical considerations associated with this technique. Zhao *et al*. (2015) generated a 3-D reconstruction of Guqin cavity through Mimics software of a surface rendering method and converted the 2-D CT tomography images into three-dimensional images. This method showed the complete interior structural form in Guqin, and the parameters of cavity dimensions were obtained. (Zhao *et al*. 2015). However, the internal visualization was limited to a direction of CT tomography.

Some other studies showed that CT can be applied in other wood materials, bamboo, and metal. Li *et al*. (2013) present a combined X-ray CT method and an adapted version of the electrical resistance MC measurement method for detailed studies on MC distribution in wood products. Johnson *et al*. (2014) studied the number of connected vessels in larger samples by using high-resolution computed tomography and three-dimensional (3-D) image analysis. Carolina *et al*. (2015) developed a methodology for modelling spatial variations of relative wood density using variograms on XRCT images. Wang *et al*. (2016) used X-ray computed tomography (CT) to study the properties and structures of bamboo materials. Li *et al.* (2017) introduced computed tomography (CT) scanning technology which was employed to observe the morphology of damage degrees as well as to explore the mechanism of degradation behavior of BLVL. Wu and Withers (2017) introduced the basic 3D and time-lapse (4D) tomographic methods and discussed their advantages and limitations across a range of the applications.

CT can be used to obtain high-precision 3-D models without damaging cultural wooden relics (Qiu and Zhang 2008). Dotting was used to utilize GOSAN (white light scanner) and HANDYSCAN (red light scanner) in order to scan cultural wooden relics due to their small chromatism. However, some precious cultural relics are untouchable, not to mention dotting (Zhao *et al.* 2017).

Laser scanning can be divided into white light scanning, blue light scanning, and red light scanning, and their results differ with the same equipment due to various characteristics of light sources. For example, results of white light scanning generally have the worst accuracy, while those of the other two seem similar. The authors conducted three-dimensional reconstruction and printing experiments by using GOSAN, HANDYSCAN, and COMET 6 (blue light scanner), for which the precision of the results was not as high as that produced by CT scanner. Moreover, patches are compulsory in red light scanning, usually with 4 patch points scattering in 10 cm, serving as positioning coordinates during the scanning process (Zhao *et al.* 2017). A reverse process to remove them is required after the scanning, which may cause irreversible damage to some precious cultural relics that require special operations for preservation. In addition, the laser scanning is not able to provide the internal structural information of the tested object. Comparing with 3-D scanning, the advantage of CT is that internal structure of the scanned relics can be obtained (Zhao *et al.* 2017). Taking the experiment of Noble Consort couch as an example, not only was the 3-D model obtained with as high resolution as was practical, but the internal texture of the specimen was visible. Three-dimensional tomography can obtain a clear internal structure of wood artifacts. In this experiment, for example, the three-dimensional model of the royal couch obtained was highly consistent with the physical objects, and the texture inside the wood specimen was precise. The digital model records real three-dimensional information and texture information for wood artifacts, providing important support for cultural relics restoration and restoration.

While the digital processing of cultural wooden relics can be achieved through 3-D expression and virtual display, it can also record the original 3-D information and texture information of the cultural relics through the accurate digital model. This data and modeling supports the restoration and recovery of cultural relics (Zhao *et al*. 2017).

Since ancient time, the identification of cultural relics, called "Observation", was by means of the appraiser's personal experience and moral qualities (Yue 2011; Zheng *et al*. 2014). With the development of science and technology, the craftsmanship of fake cultural wooden relics has reached its peak, which then results in difficulties in the distinction of original and fake ones by "Observation". For a long time, the identification of original and fake cultural relics has been carried out by the appraiser, while the variety in professional quality and moral levels of these appraisers greatly influence the results of the identification. Yet many cultural relics fakes are being traded in the market, such that the accuracy of their identification based on the appraiser's visual and tactile evaluation is doubtable. It is difficult to distinguish them only by eye, which makes it an urgent need to identify them with modern techniques. As a modern technological approach, CT can provide technical support for the identification and protection of cultural wooden relics.

EXPERIMENTAL

Experimental Preparation

The first step was to prepare the wooden articles. The second step was to put the prepared wooden artifacts into the CT tube. The parameter settings of the CT scan are shown in Table 1.

Table 1. Philips 16 Row CT Scan Parameters

Major Equipment	Product Parameters
Fastest Scanning Time	360:0.4 s
Number of Layers Per Scan	16
Thinnest Layer Thickness	0.75 mm
Thinnest Image Reconstruction Layer Thickness	0.6 mmu
Biggest Layer Thickness	12 mm
Image Reconstruction Speed	Transcripts/s
Scanning Visual Field	25 cm, 50 cm
Image Reconstruction Matrix	512 × 512, 1024 × 1024 (optional)
Maximum Scanning Time Per Single Spiral	100 s
Maximum Range Per Single Spiral	150 cm
Orientation	Every direction
Locating Image Length	175 cm

The third step, using MATLAB (Massachusetts, US) for image segmentation experiments in a Window 7 operating system (Washington, US) to verify the effectiveness of this method. As the fourth step in the experiments, the CT images of wooden relics were reconstructed by volume rendering and surface rendering, respectively, using the self-developed medical image system based on VTK. In the fifth step, the medical image analysis software OSIRLX (Bernex, Switzerland) was used to segment the different positions and angles.

Materials

The experimental materials used in this study included Noble Consort couch (carved piece painted decoration), size (27 cm ×11 cm × 9 cm).

3-D Visualization

The OTSU algorithm method was applied in the 3D-visualization of wooden relics due to the high similarity in grayscale of CT images produced by the objects. OTSU was originally introduced by Nobuyuki in the field of image processing in the late 1970s for the analysis of binary images, which was usually used to segment CT images in a region-based situation. Apart from the grayscale, some objects in the cultural wooden relics were in mortise and tenon connections, which fits the situation of OTSU method (Mehmet and Bulent 2004).

The OTSU method is widely used in the field of medical image segmentation. It possesses some advantages such as high calculating speed and positioning accuracy. But it is innately susceptible to noise, which can result in either under-segmentation or over-segmentation (Cai *et al*. 2017; Farag *et al*. 2017; Shahzad *et al*. 2017; Tovia-Brodie *et al*. 2017; Xiong *et al*. 2017; Yan *et al*. 2017). Therefore, the present work combined multiple methods to overcome this drawback; these methods and the processes are shown in Fig.1. Firstly, the CT images of cultural wooden relics were filtered and smoothed. Then the smoothed images were segmented by using OTSU method. Finally, the 3D-reconstructed images were obtained based on the segmented CT images.

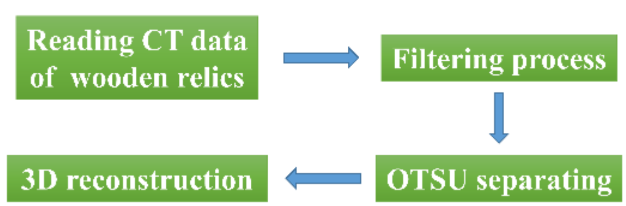

Fig. 1. Flowchart of 3-D reconstruction of CT image

Total Variation Filtering

There are many non-linear filtering methods, such as the classic median filter, mean filter, and bilateral filtering (Lu *et al*. 2017). The median filter, in which the noise component is difficult to select, does not affect the output, but the speed is very slow. The mean filter is the average calculation of the noise components; therefore the output is affected by noise. The Gaussian low-pass filter can remove noise to smooth the image and can generate a blurred edge (Cai *et al*. 2017). Bilateral filtering is a compromise between the spatial proximity of the image and the similarity of the pixel values (Cai *et al*. 2004). Considering the similarity of spatial information and the gray-level similarity, it can remove noise and have features of being simple, iterative, and partial (Huang 2015; Liang *et al*. 2015; Binge *et al*. 2017; Lu *et al*. 2017; Sarrafpour *et al*. 2017; Wang et al. 2017). The model based on total variation is an optimization model that needs to be solved iteratively. Compared with the above algorithm, the total variation model has a better effect on CT images. Therefore, this model is adopted in this paper. In Eq. 1, $g(x, y)$ is the CT image with noises, $n(x, y)$ is the noise of CT image, and $f(x, y)$ is the clear image that needs to be restored, the equation is:

$$\mathrm{g}(x, y) = \mathrm{f}(x, y) + n(x, y) \tag{1}$$

According to Eq. 1, the total variation model can be expressed in Eq. 2,

$$\min_{\mathrm{f}}\left\{\lambda \int_{\Omega} |\nabla f|\, dx\, dy + \int_{\Omega} (g - f)^2\, dx\, dy\right\} \min_{\mathrm{f}}\left\{\lambda \int_{\Omega} |\nabla f|\, dx\, dy + \int_{\Omega} (g - f)^2\, dx\, dy\right\} \tag{2}$$

where λ is a smoothing coefficient in which the greater the value, the more clear recovery the smooth image has. The optimization in Eq. 2 can be adopted in the traditional gradient descent algorithm, shown in Eq. 3,

$$\frac{\partial f}{\partial t} = \lambda div \left(\frac{\nabla f}{|\nabla f|_{\varepsilon}}\right) - 2(f - g) \tag{3}$$

where *div* is the divergence operator, ε is a small positive number used to avoid the total variation non-differentiable, and t is a manually selected time step which was the value chosen to meet the conservation rate (the CFL conditions).

In addition to the gradient descent method, some fast algorithms such as split Bregman, principal dual, alternating direction multivariable, and other algorithms can also be used to deal with the total variation model. This article does not go into details of these methods.

OTSU Threshold Segmentation

The OTSU algorithm is an adaptive threshold segmentation algorithm (Ouadfel and Taleb-Ahmed 2016; Zortea *et al*. 2017). Based on the grayscale value characteristics, the image can usually be divided into the foreground and the background. If the grayscale value of the foreground and background differs greatly, the internal variance is also great. This means that the probability of segmentation error should be minimized.

Assuming that $f(x, y)$ $ff(x, y)$ $f(x, y)$ is the filtered image, its size is $M \times N$ $M \times N$. Selecting threshold to split $f(\mathrm{x, y})$ $f(x, y)$ $f(x, y)$ into foreground and background; the number of pixels in the foreground is s1$s1s1$, and the mean gray-scale is u1. The number of pixels in the background is s_2, and the mean gray-scale is u_2. The ratio of the foreground and background in the image is shown in Eqs. 4 and 5,

$$w_1 = \frac{s_1}{(M \times N)} w_1 = \frac{s_1}{(M \times N)} \tag{4}$$

$$w_2 = \frac{s_2}{(M\ x\ N)} \quad w_2 = \frac{s_2}{(M\ x\ N)} \tag{5}$$

The total gray scale of the image is shown in Eq. 6,

$$u = u_1 \times w_1 + u_2 \times w_2 u = u_1 \times w_1 + u_2 \times w_2 \tag{6}$$

and the inner variance of the image at this time is shown in Eq. 7,

$$f(T) = w_1 \times (u_1 - u_2)^2 + w_2 \times (u - u_2)^2 \tag{7}$$

Through all the thresholds to find the T results in the largest intra-variance $f(\mathrm{T})$ and is the final segmentation result.

Experimental Analysis

To verify the effectiveness of the method mentioned in Fig.1, data from CT images of the wood relic were analyzed by MATLAB on Window 7 system for image segment experiments. A Philips Brilliance 16 CT scanner was used to scan the rosewood relic, which was decorated by paint and was in a size of 27cm×11cm×9cm. The layer thickness was set as 0.75 mm, and 146 images were obtained. The 143th (Fig. 2) was taken for further processes.

De-noising

In CT scanning experiments, noise from the equipment and environment can result in unclear images. De-noising is a process that removes this noise from signals. The original CT image (without de-noising) of the rosewood relic were found to have many contour points and its gray levels were uneven. Therefore, the total variation filter was applied due to its capacity of contourlet transformation, and the outcome de-noised CT image was shown in Fig. 3. In comparison with the original image, the de-noised image had even, gray levels and clear, smooth contours.

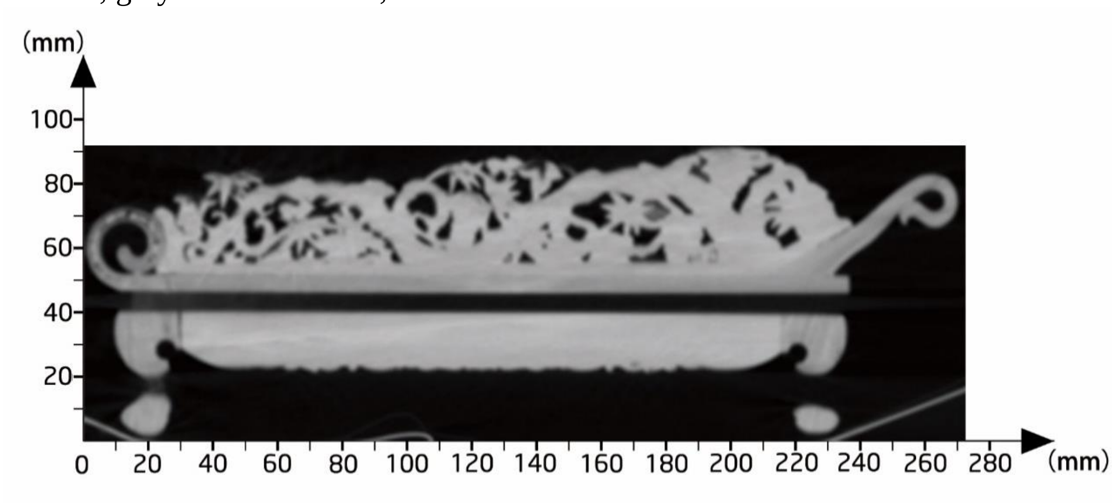

Fig. 2. Image de-noising results (Remove the image in the digital experiment and the transmission process is often influenced by the imaging device and the external environmental noise impact noise)

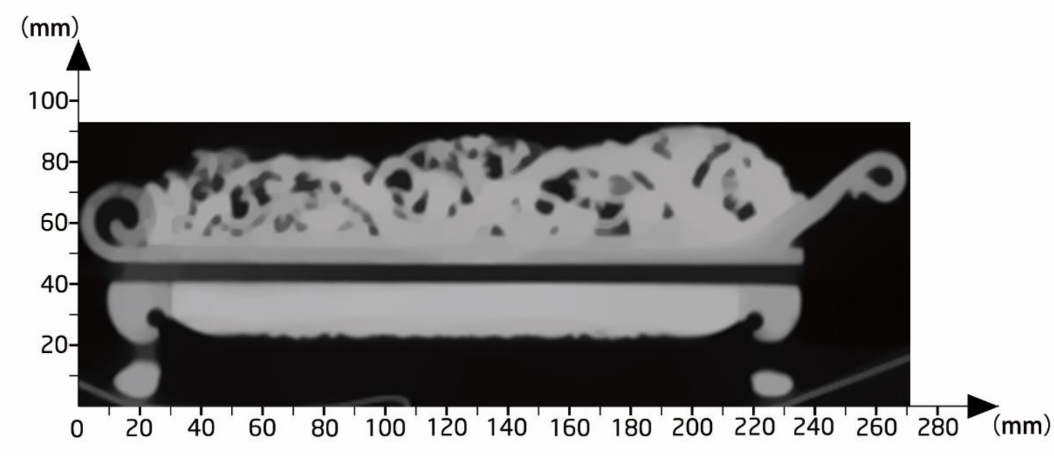

Fig. 3. Filtered results (Image filtering, as far as possible to retain the details of the image characteristics of the target image to suppress the noise, the effect of its processing will directly affect the subsequent image processing and analysis of the effectiveness and reliability.)

Image filtering

Wave filtering is an operation that filters the frequency of a particular band in the signal, and it is important in suppressing and preventing interference. Wave filtering is divided into classical filtering and modern filtering. In considering the specificity of the various filters, one of the classical filtering, the bilateral filter was applied in this experiment. Considering spatial information and gray level similarity, it can preserve the edge and eliminate the noise, and has the character for simple, non-iterative part (Cai *et al*. 2004; Yu *et al*. 2009). This paper uses bilateral filter for image filtering.

Image segmentation

Image segmentation was used to divide the image into a number of specific, unique properties of the region and the target image. Figure 4 shows the results of the segmentation. The OTSU algorithm was used to separate wooden relics and non-wooden relics, shown in Fig. 5.

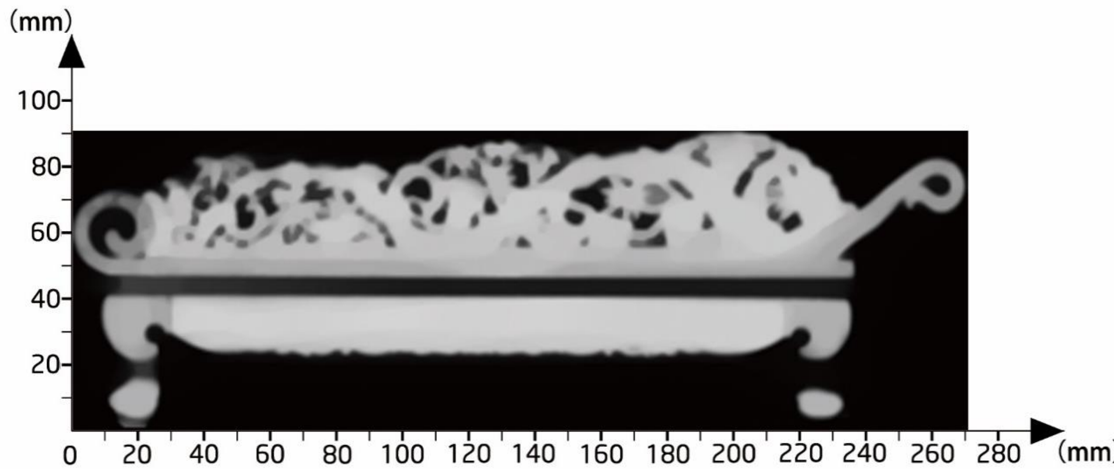

Fig. 4. Image segmentation results (Image segmentation is to divide the image into a number of specific, unique properties of the region and the target image)

3-D Reconstruction

The 3-D reconstruction refers to the establishment of a mathematical model of the subject in computer systems. This technology is the basis of dealing, manipulating, and analyzing objects in a computer system, which is also a key technology to expressing virtual reality. The methods of 3-D reconstruction mainly include a surface rendering method and a volume rendering method. The surface rendering method is to build a geometric model of the surfaces of a subject, and to manifest the model by using computer graphics technology. The results of this is shown in Fig.7. The volume rendering method is to display the images by applying a 3-D discretely sampled data set (3-D scalar field), in which the geometric model is not required. In this study, the marching cubes algorithm in the medical image reconstruction was used for volume rendering. The results are shown in Fig. 8. The advantages of volume rendering is that the internal structure can be reconstructed. The internal structure is shown in Figs. 10, 11, and 12.

The supplemented processes are as shown below:

(1) The 3D models (saved as DICOM file) of the wood object obtained from the CT scanning was imported to Mat lab.

(2) Each image was filtered in Mat lab to de-noise.

(3) Images were then converted to '.bmp' format after segmenting by OTSU algorithm.

(4) The converted '.bmp' images were used to conduct 3D reconstruction by using marching cubes algorithm in TM-Mis, an image diagnostic software. The details were shown in the next process below.

(5) Surface rendering and volume rendering were conducted in TM-Mis.

The parameter settings of surface rendering are shown in Fig. 5, where the smoothness value ranged from 1 to 100, and the pixel value ranged from -1000 to 1000. Particularly, the closer the smoothness value is to 100, the smoother the 3D model can be printed; and the closer the pixel value is to -1000, the finer the images are in details. On the contrary, the closer it is to 1000, the fewer the image details.

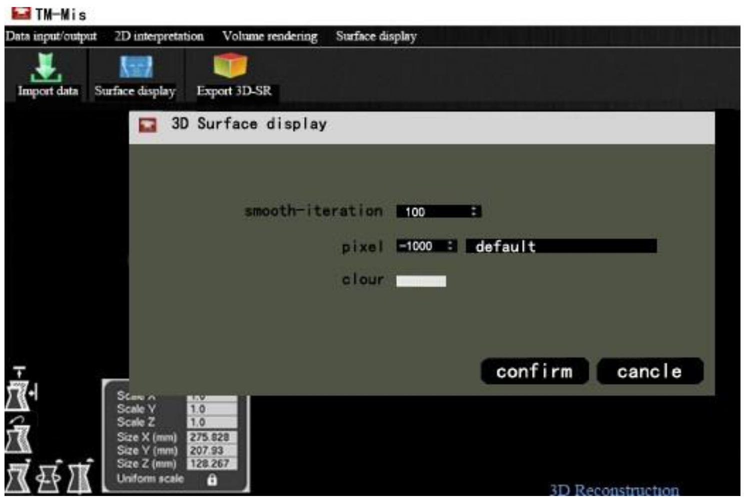

Fig. 5. 3D surface display settings

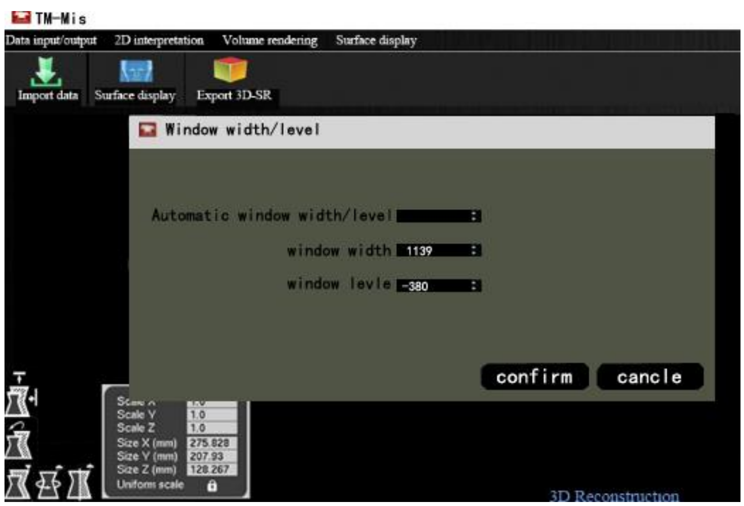

Fig. 6. 3D Volume rendering settings

The pixel value in this experiment was set to be -1000 owing to the complex inner structure of the wood material.

In the volume rendering experiment, we set the window width and window level manually, and both of these parameters ranged from -1800 to 1800. The specific values of these two parameters should be set according to the density of the specimen (wood). As long as the image of the specimen is clear, the values of window width and window level are then considered as premium. The values of these two parameters are shown in Fig. 6.

(6) The processed images were saved as ‘stl’ format for 3D printing.

In the experiments, the CT images of wooden relics were reconstructed by volume rendering and surface rendering, respectively, using the self-developed medical image system based on VTK (Visualization tool kit, an open source software system, which is widely applied in three-dimensional graphics, image processing and visualization). The results of the 3-D reconstruction are shown in Figs. 7 and 8.

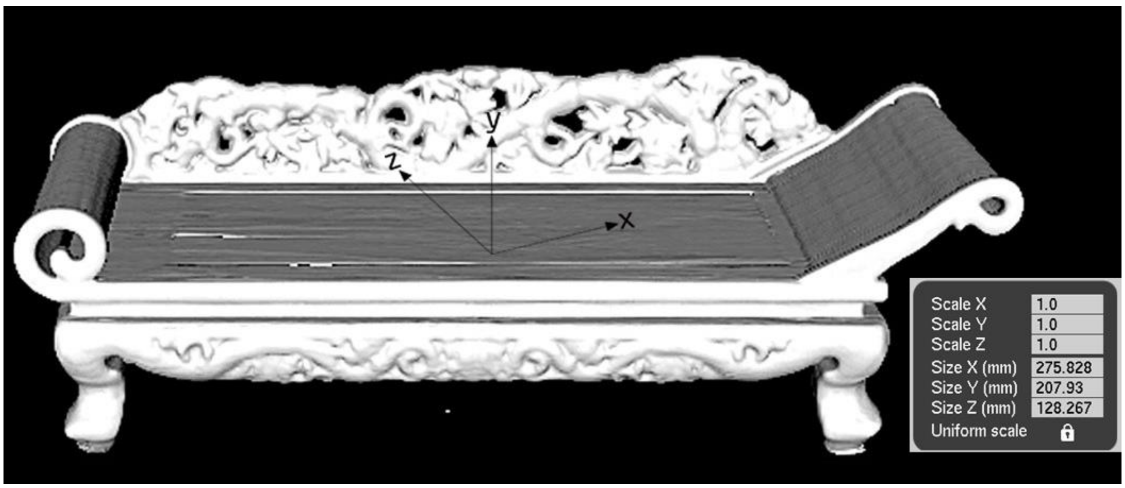

Fig. 7. Surface rendering results

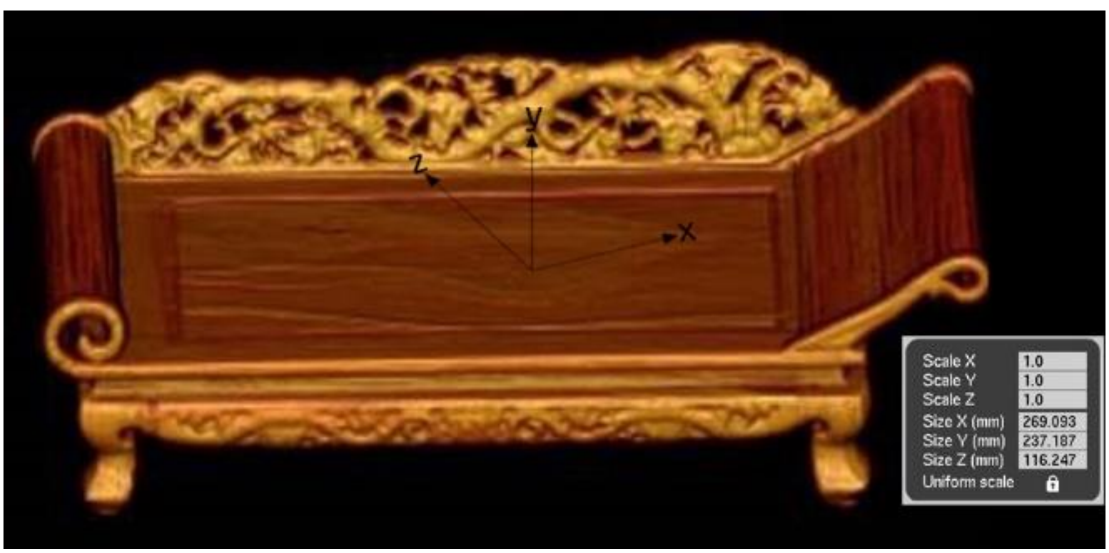

Fig. 8. Volume rendering results

RESULTS AND DISCUSSION

By setting the parameters of the window width and the window levels, the adjusted results of the wood density parameters of the Noble Consort couch were obtained, as shown in Table 2. As shown in Fig. 9, there were three kinds of wood with different densities used in the Noble Consort couch, the density of the wood in the backrest and frame structure was the highest, then the seat, and that in the curl-shaped ends possess the lowest density. Currently, wood species are mainly identified through the form of slices, while the identification of cultural relics are not allowed to be touched or damaged. First, a series of CT experiments were collected to identify the density of different wood species. According to the density value, the wood density database for cultural relics was established in order to provide supplementary data support.

Table 2. Noble Consort Couch Parameters and Density Values Change List

The Parameter of Window and Window Width	According to the Change of Density Value	The Parameter of Window and Window Width	According to the Change of Density Value
WL: 0 WW:1000	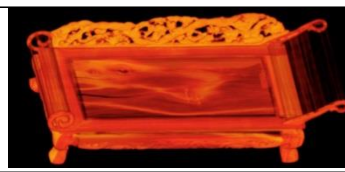	WL:200 WW:1000	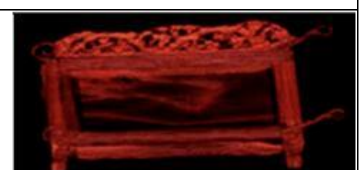
WL:50 WW:1000	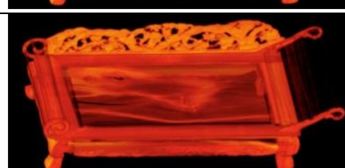	WL:250 WW:1000	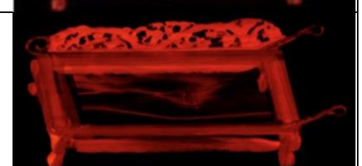
WL:100 WW:1000	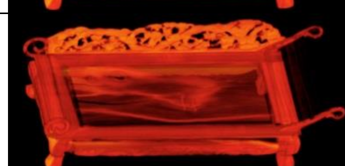	WL:300 WW:1000	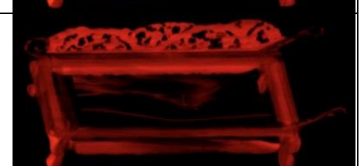
WL:150 WW:1000	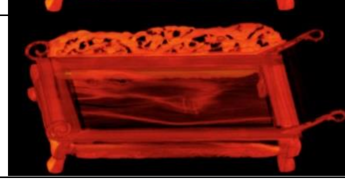	WL:350 WW:1000	

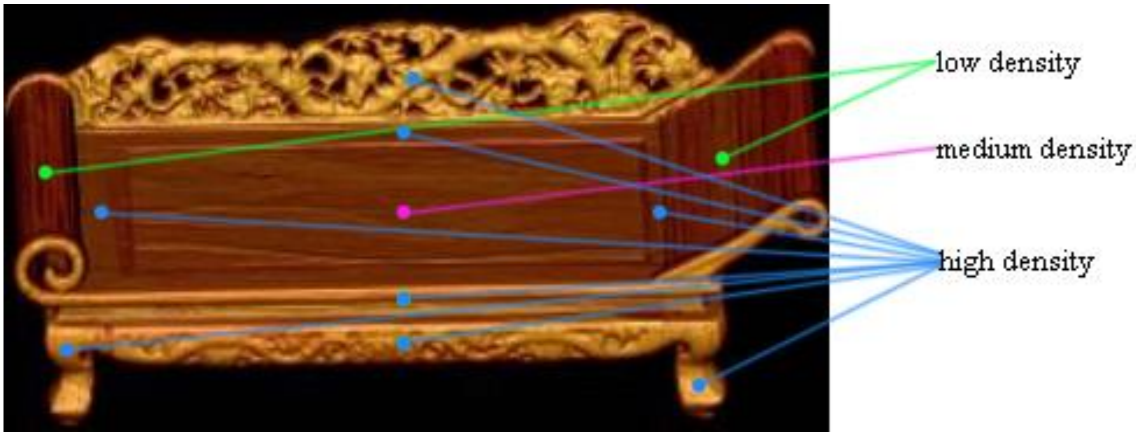

Fig. 9. Component density labeling diagram

Fig. 10. Location of the cross-cut wood texture map

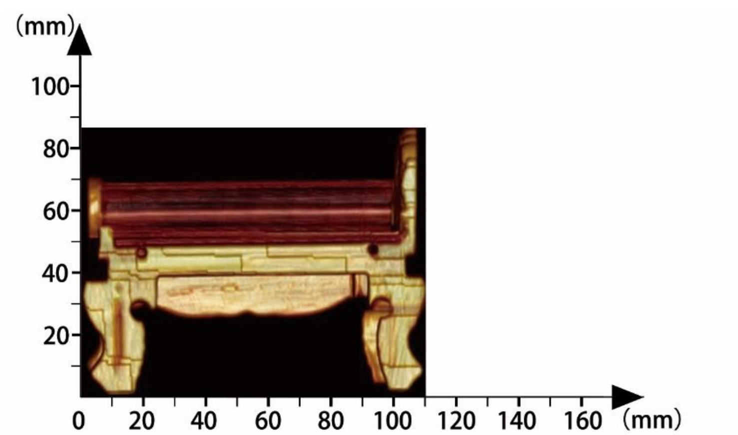

Fig. 11. Vertical couch wood texture map of the right side of Noble Consort couch

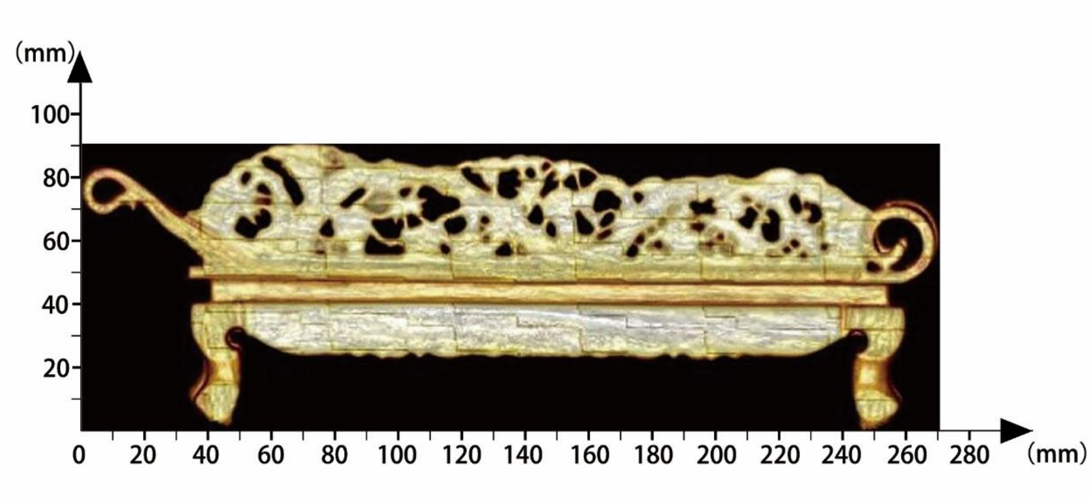

Fig. 12. Vertical couch wood texture map of the backrest of Noble Consort couch

Secondly, on the basis of volume rendering, the wooden artifacts could be graphically divided at any angle and any position. In the segmentation of the picture, the wood texture is clearly observed. The experimental results are shown in Figs.10, 11, and 12.

More importantly, accurate non-destructive testing of cultural relics can be carried out through experiments. The properties of wood as a bio-polymer material will change over time. There are a large number of cultural wooden relics that exist all over the world. They have survived hundreds to thousands of years, especially in China, South Korea, Japan, and other Asian regions where ancient buildings with wooden structures existed. Due to natural erosion and man-made impacts, there are damages on the ancient buildings from worms, cracks, erosion, distortion, and so on. The beams, columns, purlin, Fang, and other load-bearing components often look intact, but the internal damage has already occurred. Without immediate protective intervention, a collapse of a part or even the whole ancient building could occur. Presently, the methods of stress wave reflectometry, radar ultrasonic method, 3-D stress wave tomography, and a resistance meter, which is commonly used in nondestructive testing, are physical inferences to detecting the decaying positions and the size by acoustic principle. Most of these detection methods of the shape, face, size, and other areas have stringent restrictions (Ge *et al*. 2014; Sun *et al*. 2014; Stelzner and Million 2015; Hu 2016).

The intuitional analysis and judgment cannot be made on the visualization of the inner shape of the nondestructive testing parts. In this experiment, movable CT or CT was used to obtain 3-D tomography data and an experimental analysis was conducted. Through 3-D reconstruction, the internal decay, the exact location of insect damage, size, shape, and other specific information of ancient cultural wooden relic components were observed. Effective cultural relic protection methods were made and a scientific, effective, and reliable technical support for cultural relic protection was provided.

CONCLUSIONS

1. Three-dimensional computed tomography (CT) can be used to visualize the complex wooden structures of crafts through computer, which can help experts better understand the internal structures of wooden artifacts.
2. From the comparison of the density and shape of wood, it is possible to identify tree species which provides a new method for the identification of wooden artifacts.
3. With the use of professional 3-D reconstruction software to import fault data, the 3-D model can be generated directly and the model can be used as the premise of VR technology. It also plays an important role in museums and other popular science exhibitions by allowing visitors to see and understand the printed 3-D models at any time.
4. However, many facts contribute to the limited application of 3-D computed tomography (CT). For example, the requirements of professional staff participation in the printing process and in the current 3-D reconstruction, the high cost of CT machines, the position immobility of CT machines, the inconvenience to carry CT machines, the impossibility to scan large specimens, the lack of automatic image segmentation software.
5. Due to the small size of the specimen used in this experiment, the wood textures in some parts were not particularly obvious. If used larger wood artifacts in the test, the outcome could be better.

ACKNOWLEDGMENTS

This work was supported by "State Forestry Administration Introduction Of International Advanced Forestry Science and Technology Project (948)" (2003.1-2017.12) (grant number 2013-4-06), China.

REFERENCES CITED

Binge, C., Ma, X. D., and Xie, X. Y. (2017). "Classification of visible and infrared hyperspectral images based on image segmentation and edge-preserving filtering," *Infrared Phys. Techn*. 81, 79-88.

Brodersen, C. R. (2013). "Visualizing wood anatomy three dimensions with high-resolution x-ray micro-tomography (MCT): A review," *Iawa* J 34(4), 408-424.

Cai, C., Ding, M. Y., Zhou, C. P., and Zhang, T. X. (2004). "Bilateral filtering in the wavelet domain," *Acta Electronica Sinica.* 32(1), 128-131.

Cai, K., Yang, R. Q., Chen, H. Z, Li, L. H., Zhou, J., Ou, S. X., and Liu, F. (2017). "A framework combining window width-level adjustment and Gaussian filter-based multi-resolution for automatic whole heart segmentation," *Neurocomputing* 220, 138-150.

Ekevad, M. (2004). "Method to compute fiber directions in wood from computed tomography images," *J. Wood. Sci.* 50(1), 41-46.

Farag, A., Lu, L., and Roth, H. R. (2017). "A bottom-up approach for pancreas segmentation using cascaded super pixels and (Deep) image patch labeling," *IEEE. T. Image Process.* 26(1), 386-399.

Ge, X. W., Wang, L. H., and Sun, T. Y. (2014). "Quantitative detection of Salix Matsuyama inner decay based on stress wave and resist graph techniques," *China Forest Sci. Technol.* (in Chinese) 28(5), 87-91.

Hu, F. (2016). "The significance and feasibility of 3D model reconstruction of painted pottery wares cultural relics Yuhui Village site of Bengbu as an example," *China Ceram* (in Chinese) 52, 84-88.

Huang, C. T. (2015). "Bayesian inference for neighborhood filters with application in denoising," *IEEE. T. Image Process.* 24(11), 4299-4311.

Johnson, D. M., Brodersen, C. R., Reed, M., Domec, J. C., and Jackson, R. B. (2014). "Contrasting hydraulic architecture and function in deep and shallow roots of tree species from a semi-arid habitat," *Annals of Botany* 113(4), 617-627.

Kak, A. C., and Slaney, M. (1988). *Principles of Computerized Tomographic Imaging*, IEEE Press, New York.

Li, H. D., Chen, F. M., and Xian, Y. (2017). "An empirical model for predicting the mechanical properties degradation of bamboo bundle laminated veneer lumber (BLVL) by hygrothermal aging treatment," *Eur. J. Wood Prod*. 75(4), 553-560.

Li, W., Bulcke, J. V. D., Windt, I. D., Loo, D. V., and Dierick, M. (2013). "Combining electrical resistance and 3-D X-ray computed tomography for moisture distribution measurements in wood products exposed in dynamic moisture conditions," *Build Environ*. 67(9), 250-259.

Lu, X. Q., Liu, X. H., and Deng, Z. G. (2017). "An efficient approach for feature-preserving mesh denoising," *Opt. Laser Eng.* 90, 186-195.

Lu, S. W., Hu, X. B., Wen, H., Zhang, B., and Yang, X. (2017). "Seam tracking system based on bilateral filtering algorithm," *Machinery* (in Chinese) 44(5), 11-14.

Mikolajska, A., Walczak, M., and Kaszowska, Z. (2012). "X-ray techniques in the investigation of a Gothic sculpture: The risen Christ," *Nukleonika* 57(4), 627-631.

Mehmet, S., and Bulent, S. (2004). "Survey over image thresholding techniques and quantitative performance evaluation," *J. Electron. Imaging* 13(1), 146-165.

Ouadfel, S., and Taleb-Ahmed, A. (2016). "Social spider's optimization and flower pollination algorithm for multilevel image thresholding: A performance study," *Expert Syst. Appl.* 55(C), 566-584.

Qiu, Z. W., and Zhang, T. W. (2008). "Key techniques on cultural relic 3D reconstruction," *Acta Electronica Sinica* (in Chinese) 36(12), 2423-2427.

Sarigul, E., Abbott, A. L., Schmoldt, D. L., and Aramanc, P. A. (2005). "An interactive machine-learning approach for defect detection in computed tomography (CT) images of hardwood logs," in: *Proceedings of Scan Tech 2005 International Conference*, Southern Research Station, Las Vegas, Nevada, 15-25.

Sarrafpour, S., Adhi, M., Zhang, J. Y., Duker, J. S., and Krishnan, C. (2017). "Choroidal vessel diameters in pseudo-exfoliation and pseudo-exfoliation glaucoma analyzed using spectral-domain optical coherence tomography," *J. Glaucoma*, 26(4), 383-389.

Schmoldt, D. L., Occena, L. G., Abbott, A. L., Lynn, A., and Gupta, N. K. (1999). "Nondestructive evaluation of hardwood logs: CT scanning, machine vision and data utilization," *Nondestruct. Test. Eva.* 15(5), 279-309.

Shahzad, R., Bos, D., Budde, R., Pellikaan, K., Niessen, W. J., Vander, L. A., and Van, W. T. (2017). "Automatic segmentation and quantification of the cardiac structures from non-contrast-enhanced cardiac CT scans," *Phys. Med. Biol.* 62(9), 3798-3813.
Stelzner, J., and Million, S. (2015). "X-ray computed tomography for the anatomical and dendrochronological analysis of archaeological wood," *J. Archaeol. Sci.* 55, 188-196.
Sun, X. E., Zhang, D. H., and Sun, X. P. (2014). "Application of 3D digital reconstruction in the repair of bronze ware," *J. Graph.* (in Chinese) 35(6), 912-919.
Tovia-Brodie, O., Belhassen, B., Glick, A., Shmilovich, H., Aviram, G., Rosso, R., and Michowitz, Y. (2017). "Use of new imaging CARTO® segmentation module software to facilitate ablation of ventricular arrhythmias," *J. Cardiovasc. Electr.* 28(2), 240-248.
Wang, J., Wu, J. J., and Wu, Z. S. (2017). "Bilateral filtering and directional differentiation for Bayer demosaicking," *IEEE. Sens. J.* 17(3), 726-734.
Wang, Q. P., Liu, X. E., and Zhang, G. L. (2016). "Rapidly detection for moso bamboo density under different moisture condition based on X-CT technology," *Spectroscopy and Spectral Analysis* 36 (6), 1899-1903.
Wei, Q., Brigitte, L., and Rocque, L. (2011). "On the use of X-ray computed tomography for determining wood properties: A review," *Can. J. Forest. Res.* 227(41), 2120-2140.
Xiong, G. L., Sun, P., Zhou, H., and Ha, S. (2017). "Comprehensive modeling and visualization of cardiac anatomy and physiology from CT imaging and computer simulations," *IEEE. T. Vis. Comput. Gr.* 23(2), 1014-1028.
Yan, D. M., Zhang, Z. H., and Luo, Q. M. (2017). "A novel mouse segmentation method based on dynamic contrast enhanced Micro-CT images," *Plos One* 12(1), e0169424.
Yu, H. C., Zhao, L., Wang, H. X. (2009). Image denoising using trivariate shrinkage filter in the wavelet domain and joint bilateral filter in the spatial domain. *IEEE Transactions on Image Processing* 18(10), 2364-2369.
Yue, F. (2011). "Cultural relics identification and related study," *Journal of National Museum of China* (in Chinese) 100(11),148-156.
Zhao, D. D., Liu, X. E., and Yang, S. M. (2015). "Study on non-destructive testing of Guqin interior structure based on computed tomography," *Spectrosc. Spect. Anal.* 35(12), 3519-3523.
Zhao, G. L., Deng, Z. J., Shen, J., Qiu, Z. W., and Huang, J. (2017). "Three-dimensional reconstruction of wood carving cultural relics based on CT tomography data," 3rd International Conference of Pioneer Computer Scientists, Engineers, and Educators, ICPCSEE 2017, Changsha, China. Data Science - 3rd International Conference of Pioneering Computer Scientists, Engineers and Educators, ICPCSEE 2017, Proceedings, Springer Verlag, 462-471.
Zheng, R. L., and Mei, J J. (2014). "Review of professional ethics problem involved in the authentication," *Journal of Hunan University of Science & Technology (Social Science Edition)* (in Chinese) 17(2), 50-55.
Zortea, M., Flores, E., and Scharcanski, J. (2017). "A simple weighted thresholding method for the segmentation of pigmented skin lesions in macroscopic images," *Pattern Recogn.* 64, 92-104.

Article submitted: Sept. 8, 2017; Peer review completed: Nov. 18, 2017; Revised version received: Dec. 21, 2017; Accepted: Jan. 3, 2018; Published: Jan. 16, 2018.
DOI: 10.15376/biores.13.1.1548-1562